




A One-pot-synthesized Double-layered Anticoagulant Hydrogel Tube

SUN Di^{1,2#}, GAO Wenqing^{3,4#}, WU Peng^{3,4}, LIU Jie⁵, LI Shengmei²,
LI Shilin², YU Meili^{3,4}, NING Meng^{3,4}, BAI Ru², LI Tong^{3,4},
LIU Ying^{1,2} and CHEN Chunying^{1,2}

Received July 16, 2021
Accepted August 16, 2021
© Jilin University, The Editorial Department of Chemical Research in Chinese Universities and Springer-Verlag GmbH

Extracorporeal membrane oxygenation (ECMO) has emerged as a viable treatment in severe cases of acute respiratory distress syndrome, acute respiratory failure, and adult respiratory distress syndrome. However, thromboembolic events stemming from the use of ECMO devices results in significant morbidity and mortality rates; the inner surface of the ECMO tubing comes into contact with the blood and can readily initiate coagulation. In addition, the tubing needs to be continually replaced due to thromboses on the inner tube wall, which not only increases the risk of infection but also the economic burden. Despite considerable effort, a surface modification strategy that effectively addresses these challenges has not yet been realized. In this study, we developed an integrated hollow core-shell-shell hydrogel tube of gelatin/alginate/acrylamide-bacterial nanocellulose (GAA) that meets the anticoagulant requirements for the inner tubing layer as well as the highly elastic soft material needed for the outer layer. Using static blood from healthy volunteers, we confirmed that the platelets or coagulation is not stimulated by the GAA tubing. Importantly, experiments with dynamic blood also demonstrated that the inner layer of the tubing does not elicit blood clotting. The one-pot-synthesized process may provide guidance for the design of anticoagulation tubes used clinically.




Keywords Hydrogel; Extracorporeal membrane oxygenation (ECMO) tube; Coagulation; Core-shell-shell

1 Introduction

Extracorporeal membrane oxygenation (ECMO) is an extracorporeal lung assist technique used to partially or completely replace the cardiopulmonary function of patients

and gain valuable time for the treatment of primary disease. During the COVID-19 pandemic, ECMO played an important role in the treatment of severe cases of acute respiratory distress syndrome^[1], systemic inflammatory response syndrome^[2], acute respiratory failure^[3], adult respiratory distress syndrome^[4], sepsis^[5], and multiple organ failure^[6]. The anticoagulation activity and biocompatibility of the blood extracorporeal circulation circuits are critical factors in the treatment's success. Coating technologies can improve the impact of the surface on coagulation^[7,8] and mitigate systemic inflammatory response after surgery^[9–11]. Nonetheless, the inner surface of the coated ECMO tubing differs considerably from the surface of the vascular endothelium. When the ECMO tubing contacts a blood vessel, it will trigger both coagulation and inflammatory cascades because of desquamation and thrombus formation at the coating, objectively limiting widespread application of ECMO tubing.

In consideration of the above limitations, development of the following key features is critical to improvement of ECMO: (1) generation of an inner surface with a stronger anticoagulation effect; (2) effectively preventing the desquamation of the inner layer. Blood coagulation is a complex cascade of processes, by which blood clots form through the activity of coagulation factor proteins^[12]. To prevent clotting, a coating of the artificial anticoagulant, heparin, is widely used on the inner wall of ECMO tubing. Certain polysaccharides exhibit a similar anti-coagulatory mechanism to heparin and have the potential to be developed into natural anticoagulant drugs and substitutes for heparin^[13]. Sodium alginate is chosen for a non-toxic natural polysaccharide material, combining with calcium (coagulation factor IV) being an important component in clotting for anticoagulant function^[14]. Thus, an inner layer of calcium alginate when the sodium alginate solutions are extruded into a calcium chloride to produce the egg-box model hydrogel may be a viable, low-cost strategy. In addition, a method of sacrificial core materials can be used to construct a hollow core, calcium alginate hydrogel^[15], as acrylamide-calcium alginate hydrogels have been shown to possess excellent mechanical properties and biocompatibility^[16].

 LI Tong
litong3zx@sina.com
 LIU Ying
liuy@nanocr.cn
 CHEN Chunying
chenchy@nanocr.cn

These authors contributed equally to this work.

1. GBA Research Innovation Institute for Nanotechnology, Guangzhou 510700, P. R. China;

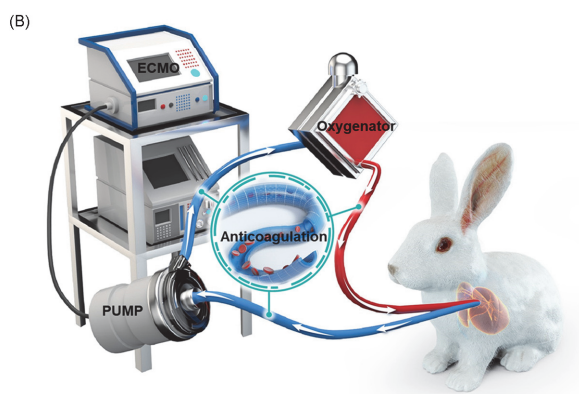
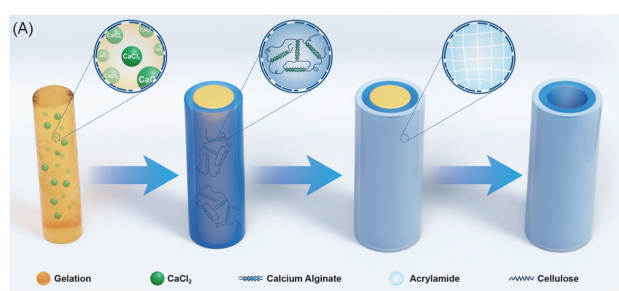
2. CAS Key Laboratory for Biomedical Effects of Nanomaterials and Nanosafety & CAS Center for Excellence in Nanoscience, National Center for Nanoscience and Technology of China, Beijing 100190, P. R. China;

3. Department of Cardiac Center, Tianjin Third Central Hospital, Tianjin 300170, P. R. China;

4. Tianjin Key Laboratory of Extracorporeal Life Support for Critical Diseases, Tianjin 300170, P. R. China;

5. Department of Vascular and Endovascular Surgery, Chinese PLA General Hospital, Beijing 100853, P. R. China

In the present study, we prepared double layer, hollow hydrogels, as illustrated in Scheme 1. A hydrogel core undergoes gelation with CaCl_2 , which forms a scaffold at $4\text{ }^\circ\text{C}$ and then melts at $60\text{ }^\circ\text{C}$ to form a hollow tube. We used calcium alginate as the inner tube so as to provide anticoagulant properties *via* the alginate chelate calcium in the blood to the double-layer gelatin/alginate/acrylamide-bacterial nanocellulose (GAA) hydrogel tube. Acrylamide/bacterial nanocellulose was used to enhance the stiffness of the multilayer hydrogel tube by atom transfer radical polymerization. The one-pot-synthesized GAA hydrogel tube in the inner layer is a suitable candidate not only for ECMO tubing but also other tubing that requires anticoagulant properties, such as artificial blood vessels and stents.



Scheme 1 Schematic illustration of the synthesis(A) and use of the anticoagulant ECMO tube

2 Experimental

2.1 Materials

Sodium alginate was purchased from Lyntech, Beijing, China. Acrylamide was purchased from Aladdin, Shanghai, China. *N,N'*-Methylenebisacrylamide(97%) was purchased from Alfa Aesar, China. Calcium chloride was purchased from Beijing Chemical Reagent Company, China. *N,N,N',N'*-Tetramethylethylenediamine(TEMED) was purchased from J&K Scientific, China. Phosphate buffered saline(PBS) was purchased from Biotopped Company, China. Dulbecco's modified Eagle medium(DMEM) and penicillin-streptomycin were purchased

from Gibco, USA. Fetal bovine serum was purchased from Hyclone, USA.

2.2 Preparation of the GAA Hydrogel Tube

Gelatin and 0.05 mol/L CaCl_2 were dissolved in 100 mL of deionized water at $60\text{ }^\circ\text{C}$. Next, the solution was transferred into tubular molds. After gelation at $4\text{ }^\circ\text{C}$ for 30 min , the gelatin was removed from the mold. The obtained gelatin core was then immersed in different alginate solutions with different concentrations[0.5%(mass fraction) alginate, GAA 0.5 hydrogel tube; 0.75% alginate, GAA 0.75 hydrogel tube; 1% alginate, GAA 1.0 hydrogel tube; 1.25% alginate, GAA 1.25 hydrogel tube; 1.5% alginate, GAA 1.5 hydrogel tube]. After 20 min , the core-shell tubular hydrogels were obtained. Next, 4.2 g of acrylamide(AA), 2.3 g of bacterial cellulose(BC), 0.006 g of *N,N'*-methylenebisacrylamide(BIS), and 0.02 g of potassium persulfate(KPS) were added to 10 mL of deionized water and mixed by a magnetic bar until all components fully dissolved as a pre-solution. In order to form a flexible outer layer of AA-BC, the core-shell tubular hydrogel tube was put in the pre-solution for 10 min . Finally, the gelatin/alginate/AA-BC hydrogels were placed into a $60\text{ }^\circ\text{C}$ oven to remove the gelatin core, yielding the two-layer hydrogel tube.

2.3 Compatibility of the GAA Hydrogel Tube

Human umbilical vein endothelial cells(HUVECs) were obtained from the American Type Culture Collection(ATCC) and cultured with DMEM containing 10%(volume fraction) fetal bovine serum and 1%(volume fraction) penicillin-streptomycin at $37\text{ }^\circ\text{C}$ with $5\%\text{ CO}_2$. The cytocompatibility of the hydrogels was determined by a direct contact method between the hydrogels and HUVECs. HUVECs were seeded on the inner surface of 0.1 g of GAA hydrogel tubes at a density of $5\times 10^4\text{ cells/cm}^2$ in 24-well plates and incubated for 1 d . The cell counting Kit-8(CCK-8) was used to evaluate cell viability. Briefly, solutions of 2 mmol/L propidium iodide(PI) and 4 mmol/L fluorescein diacetate(FDA) in PBS were used to treat the samples for 30 min at $37\text{ }^\circ\text{C}$, after which the samples were washed with PBS and then analyzed using a multi-beam laser confocal imaging system(UltraVIEW VoX, PE, Germany), with excitation wavelengths of 561 nm for PI and 488 nm for FDA^[17].

2.4 Properties of the GAA 1.0 Hydrogel Tube

The internal and external morphologies of the samples were detected after complete lyophilization for 12 h using a scanning electron microscope(SEM, HITACHI SU8010, HITACHI, Japan). Micro-CT images of the GAA hydrogel tube

were acquired using X-ray phase contrast imaging with a 128-channel TFT array (Carl Zeiss X-ray, Zeiss Xradia 520, Zeiss, Germany). The tube voltage of the Zeiss Xradia 520 Versa was set to 80 kV. After scanning, the acquired radiography images were reconstructed into a 3D volume using the ZEISS XMR Reconstructor software. The storage modulus and loss modulus were measured using a Rheometer (Rheometer, Malven Kinexus Pro+, UK) with a flat plate sensor system (radius, 10 mm) to investigate the rheological properties of the GAA 1.0 hydrogel tube.

2.5 Animals

Large-eared white rabbits were acquired from the Animal Experimental Center of Nongong (Beijing) Life Science & Technology Company (Beijing, China). All experimental protocols were approved by the Animal Care and Use Committee of the Animal Experimental Center of Nongong (Beijing) Life Science & Technology Company (202006001). All animals were housed in a temperature-controlled, ventilated, and standardized disinfected animal room, and were allowed to acclimatize, without handling, for a minimum of 1 week before the start of experiments.

2.6 Skin Irritation Test

The backs of rabbits were used as the test region, and then were shaved, skinned, and disinfected with 75% ethanol. The extract solution of the GAA 1.0 hydrogel tube in saline or sesame oil was dripped onto a 0.5 mL/(2.5 cm×2.5 cm) gauze block. The histology of the skin was observed after HE staining on days 1, 2, and 3 after treatment.

2.7 *In vivo* Transplantation

Rabbits were initially anesthetized by intramuscular injection with ketamine (30 mg/kg). Tracheal intubation and assisted ventilation were performed. Peripheral vein access was established in the left ear vein, and the fluid drip rate was maintained at 10 mL·kg⁻¹·h⁻¹. An arteriovenous extracorporeal circulation was established through the left carotid artery of the rabbit. The right carotid artery was exposed and completely dissociated. A GAA 1.0 hydrogel tube (2 cm-long) with the same inner diameter as the rabbit carotid artery (about 1.5 mm) was connected *via* two carotid artery cannulas. The blood was allowed to circulate through the in GAA 1.0 hydrogel tube for 5 min. After the experiment, the animals are euthanized with intravenous pentobarbital (130 mg/h). The activated partial thrombin time (APTT), thrombin time (TT), prothrombin time (PT), and fibrinogen content (Fg) of

the platelet-poor plasma (PPP) were measured three times before and after experiment with an automated blood coagulation analyzer (Diagnostica Stago, STA-R Evolution, France).

2.8 Thrombus Adhesion

A drop of fresh whole rabbit blood was deposited onto a 1 cm×1 cm control ECMO tube or GAA 1.0 hydrogel tube and held for 5 min at 37 °C. The sample was washed 3 times with PBS and fixed using glutaraldehyde (2.5%, mass fraction). After ethanol gradient treatment and drying under vacuum, the surfaces of the tubes were examined by SEM^[17].

2.9 Blood Compatibility Assessment of Human Blood

Fresh whole blood was obtained from Tianjin Third Central Hospital, China using standard vacuum blood collection tubes. The procedure was approved by the Hospital's Human Ethics Committee (IRB-2020-025-01). The blood was centrifuged at 3000 r/min for 10 min. The lower layer of supernatant, PPP, was used to assess blood clotting time. And 0.5 cm×0.5 cm pieces of GAA 1.0 hydrogel tubes in 24-well plates were washed three times with distilled water, equilibrated with PBS for 30 min at 37 °C, and then incubated with 200 μL of PPP for 1 h at 37 °C. After the incubation, the APTT, TT, PT, and Fg of the PPP were measured three times with an automated blood coagulation analyzer (Diagnostica Stago, STA-R Evolution, France).

2.10 Platelet Adhesion Assay

Anticoagulated blood of patients (20 mL) was centrifuged at 1250 r/min for 5 min at room temperature. The upper layer of the supernatant, *i.e.*, the platelet-rich plasma (PRP), was collected, and the number of platelets was enumerated. Then 0.5 cm×0.5 cm pieces of GAA 1.0 hydrogel tubes in 24-well plates were washed three times with distilled water, equilibrated with PBS for 30 min at 37 °C, and then incubated with a 200 μL sample of PRP for 1 h at 37 °C, following which the number of adhered platelets was counted^[18].

2.11 Protein Adsorption

Pieces of GAA 1.0 hydrogel tubes (0.5 cm×0.5 cm) were immersed in a 24-well culture plate of PPP containing 3 mg/mL human serum albumin (HSA) or human protein fibrinogen (HPF) for 60 min at 37 °C. The GAA 1.0 hydrogel tubes were gently removed from the plate and rinsed three times with

PBS. A protein analysis kit, based on bicinchoninic acid (BCA), was used to determine the concentration of the proteins. The absorbance of the solution was measured at 562 nm by means of UV-Vis spectroscopy and the amount of protein was calculated from calibrations curve of free HSA and HPF^[19].

2.12 Statistical Analysis

Values were presented as the mean with standard deviation (SD). Statistical significance among the different groups was calculated using SPSS statistical software. The statistical tests conducted in this study were indicated in the figures as follows: * $P < 0.05$, ** $P < 0.01$, *** $P < 0.001$.

3 Results and Discussion

3.1 Preparation and Characterization of the GAA Hydrogel Tube

The process we developed for preparing the hollow core-shell-shell GAA hydrogel tube is shown in Fig.1(A) and (B). We used this method to produce a series of hydrogel tubes with different concentrations of alginate (0.5%, 0.75%, 1.0%, 1.25%, 1.5%) in the inner layer as well as in the sacrificial core. Of these, only the GAA 1.0 hydrogel tube (1.0% alginate) exhibited a smooth inner surface with no cell adhesion (Fig.S1, see the Electronic Supplementary Material of this paper). As shown in Fig.1(A), before the final molding, the wall thickness of the hydrogel tube is about 1.18 mm [(6.70 mm - 4.35 mm)/2]. However, the hydrogel will undergo slight shrinkage during the free radical polymerization reaction at high temperatures. The wall thickness of the final synthetic hydrogel tube is about 1.22 mm [(6.69 mm - 4.25 mm)/2]. The cross section, longitudinal section, and three-dimension morphology of the GAA hydrogel tube have a uniform and stable structure, as revealed by X-ray phase contrast imaging [Fig.1(C) and Video 1 in the Electronic Supplementary Material of this paper]. As shown in Fig.1(D), the GAA hydrogel tube has a vessel-like structure consisting of a dense inner layer, with a smooth surface, and a porous outer layer, with a rough surface. For each layer of the GAA 1.0 hydrogel tube, the storage modulus is greater than the loss modulus, thus the material exhibits the behavior of a solid. The Young's modulus of the outer layer and the entire hydrogel tube is nearly 12000 kPa without frequency [Fig.1(E)]. The fracture stress of the inner layer is only 0.5 kPa, while that of the GAA hydrogel tube including the outer layer reaches 0.22 kPa [Fig.1(F)]. The outer layer contributes more to the mechanical strength of the entire hydrogel tube, which is important for the double-layer hydrogel tube structure. The hydrogel tube has good stability,

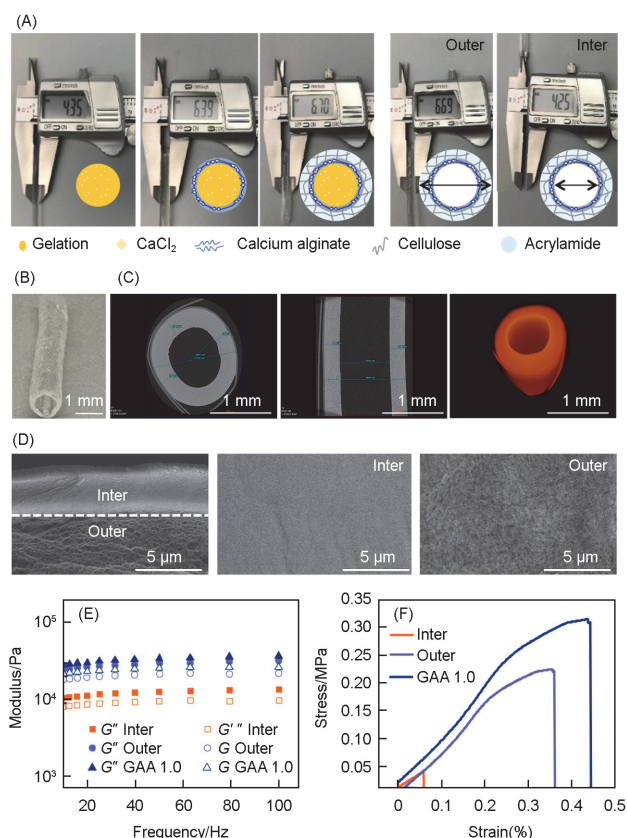


Fig.1 Characterization of the GAA 1.0 hydrogel tube

(A) Diameter of the tube at each step during the formation process, with the diameter of the core is 4.35 mm; (B) photograph of the GAA 1.0 hydrogel tube; (C) cross section (left), longitudinal section (middle), and 3D microscopic images (right) of the GAA 1.0 hydrogel tube as detected by X-ray imaging; (D) SEM images of the cross section (left), the internal surfaces (middle), and the external surfaces (right) of the GAA 1.0 hydrogel tube; (E) rheological properties of the GAA 1.0 hydrogel tube with the internal layer, external layer, and entire tube wall at 37 °C ($\epsilon = 1\%$); (F) tensile curves of the internal layer, external layer, and entire tube.

and the swelling rate is less than 10% from 1 h to 10 h (Fig.S2, see the Electronic Supplementary Material of this paper).

3.2 Anticoagulant Performance of the GAA Hydrogel Tube to Rabbit Dynamic and Static Blood

We used the GAA 1.0 hydrogel tube as ECMO tubing in the collateral circulation of rabbits to assess the material's anticoagulant properties with dynamic blood. As shown in Fig.2(A), few blood cells and proteins adhered to the inner surface of the hydrogel tube after the blood circulated in the GAA 1.0 hydrogel tube for 1 min, presumably because of the anticoagulation properties of the alginate^[20]. Furthermore, the APTT, an index of coagulation, was slightly increased (Fig.S3, see the Electronic Supplementary Material of this paper). Sodium alginate can form calcium alginate precipitates from the calcium ions in the blood, thereby preventing blood clotting.

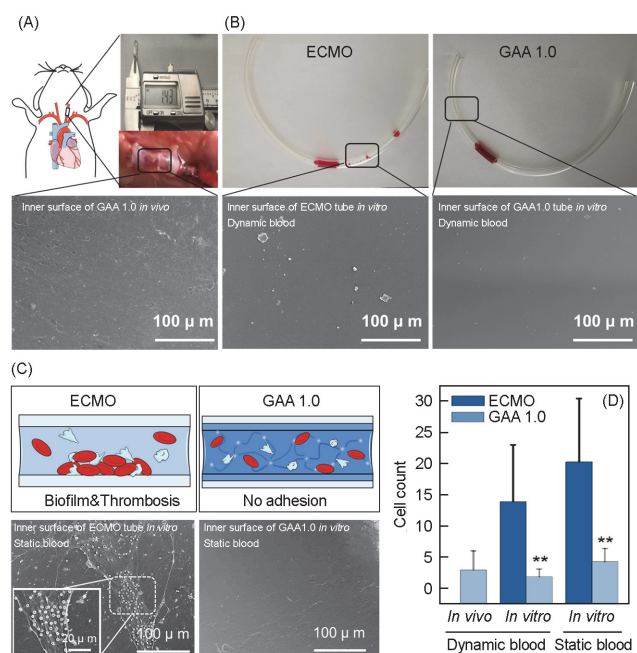


Fig.2 Anticoagulant performance of the GAA 1.0 hydrogel tube with dynamic and static blood

(A) SEM of the inner surface of the GAA 1.0 hydrogel tube after the rabbit venous extracorporeal circuit test; (B) SEM images of the inner surface of the control ECMO tube and the GAA 1.0 hydrogel tube after repeated passage of rabbit blood through the tube; (C) SEM images of the inner surface of a control ECMO tube and a GAA 1.0 hydrogel tube after a 0.5 mL of blood drop was incubated on the inner surface for 1 min; (D) quantify of the blood cell on the inner surfaces (** $P < 0.01$).

In another experiment, we placed rabbit blood into the GAA 1.0 hydrogel tube after flowing blood through the tubing repeatedly for 5 cycles *in vitro* [Fig.2(B) and Video 2 in the Electronic Supplementary Material of this paper]. Any blood proteins accumulated on the material surface are expected to alter the intercellular interaction pathways^[21] and enter the blood circulation system^[22]. We found no apparent thrombi adhering to the inner wall of the GAA 1.0 hydrogel tube by SEM. Since material from dynamic blood may not easily adhere to the inner wall of the GAA hydrogel tube, we performed a static blood experiment, in which 0.5 mL of rabbit blood was placed onto the surface of hydrogel tube, which was incubated for 1 min prior to inducing blood flow through the tubing. Thrombus formation begins with a layer of adsorbed protein after the blood contacts the surface of the tube, followed by platelet adhesion. We observed platelets and thrombi in the control ECMO group, while no adherent thrombi or platelets were detected in the GAA 1.0 hydrogel tube [Fig.2(C)]. The GAA 1.0 hydrogels has excellent anticoagulant performance compared with ECMO tube regardless of static blood or dynamic blood test [Fig.2(D)]. The quantity of adhered platelets on the inner surface of the tubing is shown in Fig.3(A), and the platelet adsorption went from (167.43±3.59) mg/cm² in the control group to (12.58±0.73)

mg/cm² in the GAA 1.0 hydrogel tube. Two plasma proteins, human serum albumin (HSA) and human protein fibrinogen (HPF), were also significant components of the adhered material on the inner tubing. Consistent with the platelet adsorption results, the adsorption of these proteins onto the GAA hydrogel tube was markedly lower than that in the control ECMO tube group [Fig.3(B) and (C)]. Taken together, these results show that the inner surface of the GAA 1.0 hydrogel tube confers significantly improved anticoagulant effects and blood compatibility.

3.3 Anticoagulation Properties of the GAA Hydrogel Tube to Human Blood

We examined the anticoagulant activity of the GAA hydrogel tubes using the hemostasis indices, APTT, TT, PT, and Fg^[23]. Wasted blood samples from healthy blood coagulation of patients were obtained using standard vacuum blood collection tubes at Tianjin Third Central Hospital. Compared with those of the control ECMO tube, the APTT and TT in the GAA 1.0 hydrogel tube group were significantly increased by 1.87- and 5.70-fold, respectively [Fig.3(D) and (E)], indicating improved anticoagulation abilities with static blood in the GAA hydrogel tube with the inner layer. No significant differences were observed in the PT (80%—120%) and Fg (2—4 g/L) [Fig.3(F) and (G)].

3.4 Cyto-compatibility of the GAA Hydrogel Tube

We assessed the cytotoxicity of the GAA hydrogel tube using the CCK-8 assay. As shown in Fig.4(A), the viability of HUVECs cultured directly on the GAA hydrogel was unaffected after 24 h. Additionally, we observed a larger number of cells proliferating on the hydrogel when the surface was rough (Fig.S1); as the percentage of calcium alginate increased, fewer cells adhered to the surface of the GAA hydrogel tube.

Skin irritation is another important possible effect factor of the GAA hydrogel tube. This occurrence can be assessed as per the National Standards in China (GB/T 16886.10-2017/ISO 10993-10:2010). We therefore performed histopathological analysis using hematoxylin and eosin (HE) staining of sections from skin harvested from rabbits after a 72 h exposure to the tubing materials. The score of the skin irritation test was 0 and the HE staining showed no untoward effects or infiltration of the skin layers, including the epidermis and subcutaneous layer [Fig.4(B)]. Together, these data demonstrate that the GAA hydrogel tube has a favorable biocompatibility.

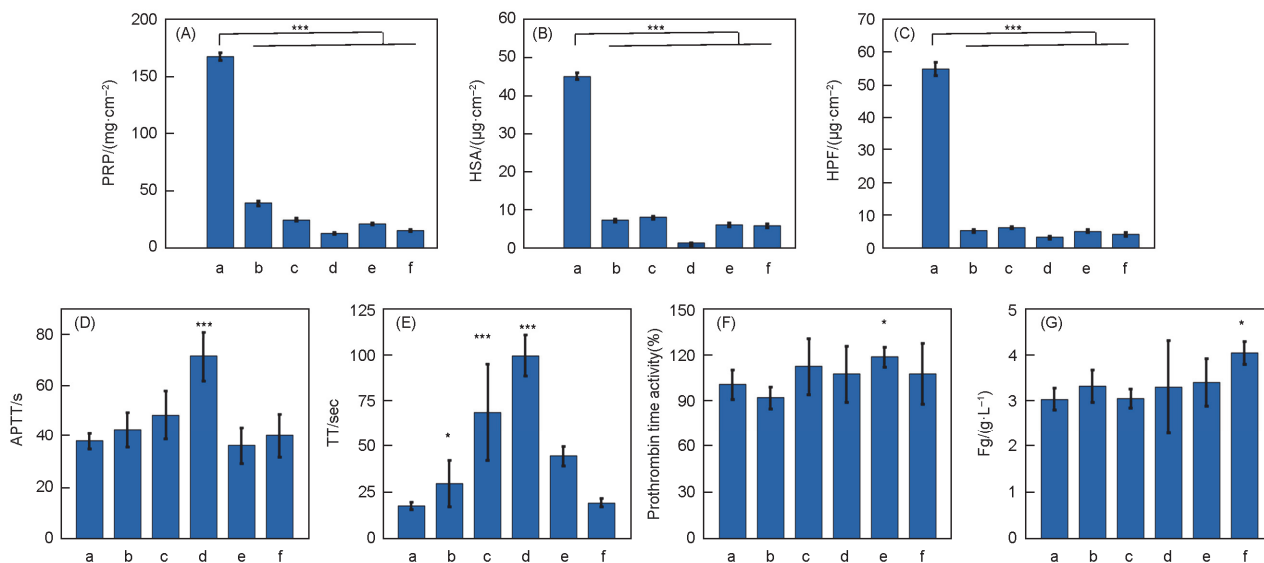


Fig.3 Coagulation function and adhesion of platelets on the inner surface of control ECMO and GAA 1.0 hydrogel tubes

a. ECMO; b. GAA 0.5; c. GAA 0.75; d. GAA 1.0; e. GAA 1.25; f. GAA 1.5. (A) Surface adsorption of platelets from human blood; (B) surface protein adsorption of HAS; (C) surface protein adsorption of HPF; (D—G) after control ECMO tubes and GAA 1.0 hydrogel tubes were expose to human blood, the activated partial thrombin time(APTT, D), thrombin time(TT, E), prothrombin time activity(F), and fibrinogen amount(Fg, G) were measured using an automated blood coagulation analyzer (***P<0.001; **P<0.01; *P<0.05; NS, not significant).

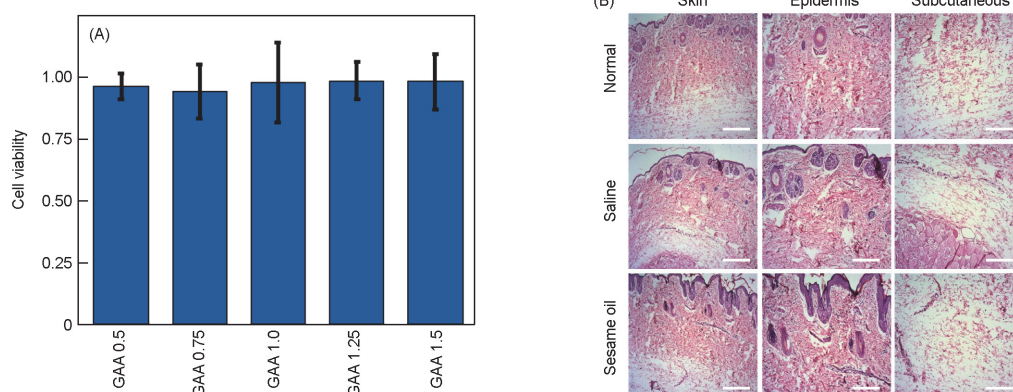


Fig.4 Biocompatibility of the GAA 1.0 hydrogel tube

(A) 24 h after seeding HUVECs on the inner surface of 0.1 g of GAA 1.0 hydrogel tube pieces, the cell viability evaluated using the CCK-8 assay; (B) histological examination of skin samples, showing the skin(scale bars=2.5 mm), and epidermis and subcutaneous layers(scale bars=100 μm), with the current standard-of-care ECMO tubing being considered to have an excellent biocompatibility.

4 Conclusions

Here we describe a one-pot synthesis of hollow polymeric hydrogels with anticoagulants. Our strategy led to the successful fabrication of GAA hydrogels with anticoagulant layers. The inner layer of the GAA hydrogel tube is highly hemocompatible and antithrombotic, as evidenced by no thrombus formation in a rabbit model of dynamic blood flow as well as with static blood. Compared with the current standard-of-care ECMO tubing, APTT and TT of human blood in the GAA 1.0 hydrogel tube were significantly increased by 1.87- and 5.70-fold, respectively. The use of a double-layered blood vessel-like structure of the hydrogel may reduce the

mortality of ECMO patients and avoid the risk of inflammatory and coagulation cascades. In addition, the strength of the outer layer of the GAA hydrogel tube can be improved in future versions of the tubing. Further, this simply method may have promising applications in other blood-contacting materials, such as bioartificial vessels and hemodialysis.

Electronic Supplementary Material

Supplementary material is available in the online version of this article at <http://dx.doi.org/10.1007/s40242-021-1267-3>.

Acknowledgements

This work was supported by the Key-Area Research and Development Program

of Guangdong Province, China(Nos.2020B0101020001, 2019B090917011), the Strategic Priority Research Program of the Chinese Academy of Sciences (No.XDB36000000), the Innovative Research Groups of the National Natural Science Foundation of China(No.11621505), the National Natural Science Foundation of China(No.31971318), the Key Fund of the Tianjin Health Commission, China(No.2014KR01), the Youth Fund of the Tianjin Science and Technology Commission, China(No.17JQJNC10000), and the Tianjin "Project+Team" Key Training Special Project, China(No.XC202040).
The authors would like to thank Prof. Yapei WANG from Renmin University of China.

Conflicts of Interest

The authors declare no conflicts of interest.

References

- [1] Hardin C. C., Hibbert K., *N. Engl. J. Med.*, **2018**, 378, 2032
- [2] Millar J. E., Fanning J. P., McDonald C. I., McAuley D. F., Fraser J. F., *Crit. Care.*, **2016**, 20, 387
- [3] Brodie D., Slutsky A. S., Combes A., *Jama.*, **2019**, 322, 557
- [4] Mendes P. V., Melro L. M. G., Li H. Y., Joelsons D., Zigaib R., Ribero J., Besen B., Park M., *Rev. Bras. Ter. Intensiva.*, **2019**, 31, 548
- [5] Bréchet N., Hajage D., Kimmoun A., Demiselle J., Agerstrand C., Montero S., Schmidt M., Luyt C. E., Lebreton G., Hékimian G., Flecher E., Zogheib E., Levy B., Slutsky A. S., Brodie D., Asfar P., Combes A., *Lancet*, **2020**, 396, 545
- [6] Sparks B. E., Cavarocchi N. C., Hirose H., *J. Heart. Lung. Transpl.*, **2017**, 36, 71
- [7] Münch F., Höllerer C., Klapproth A., Eckert E., Ruffer A., Cesnjevar R., Göen T., *Chemosphere*, **2018**, 202, 742
- [8] Fan Y., Zhang Y., Zhao Q., Xie Y., Luo R., Yang P., Weng Y., *Biomaterials*, **2019**, 204, 36
- [9] Silveti S., Koster A., Pappalardo F., *Artif. Organs.*, **2015**, 39, 176
- [10] Ontaneda A., Annich G. M., *Front. Med-PRC.*, **2018**, 5, 321
- [11] Maul T. M., Massicotte M. P., Wearden P. D., *Extracorporeal Membrane Oxygenation-Advances in Therapy*, IntechOpen, London, **2016**
- [12] Dahlbäck B., *Lancet*, **2000**, 355, 1627
- [13] Zeymer U., Rao S. V., Montalescot G., *Eur. Heart. J.*, **2016**, 37, 3376
- [14] Yu J., Su H., Wei S., Chen F., Liu C., *J. Biomt. Sci-Polym. E*, **2018**, 29, 1716
- [15] Ouyang L., Burdick J. A., Sun W., *ACS Appl. Mater. Inter.*, **2018**, 10, 12424
- [16] Zhou Y., Gui Q., Yu W., Liao S., He Y., Tao X., Yu Y., Wang Y., *ACS Biomater. Sci. Eng.*, **2019**, 5, 6311
- [17] Felgueiras H. P., Wang L. M., Ren K. F., Querido M. M., Jin Q., Barbosa M. A., Ji J., Martins M. C., *ACS Appl. Mater. Inter.*, **2017**, 9, 7979
- [18] Sivaraman B., Latour R. A., *Biomaterials*, **2010**, 31, 832
- [19] Higuchi A., Sugiyama K., Yoon B. O., Sakurai M. Hara M., Sumita M., Sugawara S., Shirai T., *Biomaterials*, **2003**, 24, 3235
- [20] Mao J. Y., Lin F. Y., Chu H. W., Harroun S. G., Lai J. Y., Lin H. J., Huang C. C., *J. Colloid. Interf. Sci.*, **2019**, 552, 583
- [21] Ge C., Du J., Zhao L., Wang L., Liu Y., Li D., Yang Y., Zhou R., Zhao Y., Chai Z., Chen C., *Proc. Natl. Acad. Sci. USA*, **2011**, 108, 16968
- [22] Du J., Gu Z., Yan L., Yong Y., Yi X., Zhang X., Liu J., Wu R., Ge C., Chen C., Zhao Y., *Adv. Mater.*, **2017**, 29, 1701268
- [23] Long H., Nie L., Xiang X., Li H., Zhang X., Fu X., Ren H., Liu W. Wang Q., Wu Q., *Biomed. Res. Int.*, **2020**, 2020, 6159720